J. Phycol. **46,** 1114–1127 (2010)

DOI: 10.1111/j.1529-8817.2010.00923.x

PHOTOPHYSIOLOGY IN TWO SOUTHERN OCEAN PHYTOPLANKTON TAXA: PHOTOSYNTHESIS OF *PHAEOCYSTIS ANTARCTICA* (PRYMNESIOPHYCEAE) AND *FRAGILARIOPSIS CYLINDRUS* (BACILLARIOPHYCEAE) UNDER SIMULATED MIXED-LAYER IRRADIANCE[1]

Matthew M. Mills,[2] *Lindsey R. Kropuenske, Gert L. van Dijken, Anne-Carlijn Alderkamp, Gry Mine Berg*

Department of Environmental Earth System Science, Stanford University, Stanford, California 94305, USA

Dale H. Robinson

Romberg Tiburon Center, San Francisco State University, Tiburon, California 94920, USA

Nicholas A. Welschmeyer

Moss Landing Marine Laboratories, Moss Landing, California 95309, USA

and Kevin R. Arrigo

Department of Environmental Earth System Science, Stanford University, Stanford, California 94305, USA

In the Ross Sea, the prymnesiophyte *Phaeocystis antarctica* G. Karst. dominates deeply mixed water columns, while diatoms dominate shallower mixed layers. Understanding what controls the dynamics of these two phytoplankton taxa is essential because they dominate virtually all coastal polar waters, have different nutrient utilization characteristics, and support dissimilar food webs. We cultured two strains of *P. antarctica* and one strain of the diatom *Fragilariopsis cylindrus* (Grunow) Willi Krieg under three dynamic irradiance regimes that simulated different mixed-layer depths and measured their photosynthetic characteristics, cellular pigment concentrations, and cellular carbon and nitrogen content. In both species, chl *a*–normalized maximum carbon uptake rate (P_m^*) and specific growth rate were highest in the deeply mixed treatment that had a dark period. In all irradiance treatments, both (P_m^*) and photosynthetic efficiency (α^*) were greater for the two *P. antarctica* strains than for the *F. cylindrus* strain. In contrast, *P. antarctica* strains were more susceptible to photoinhibition (β^*) than the *F. cylindrus* strain. When photosynthetic rates of each phytoplankton taxon were normalized by cellular particulate organic carbon (POC), the difference in the maximal photosynthetic rate (P_m^C) was generally reduced. In the dynamic irradiance treatment that simulated the shallowest mixed-layer irradiance, all three phytoplankton had similar P_m^C; however, the diatom had a 2-fold higher POC-normalized photosynthetic efficiency (α^C). Finally, we performed calculations using the measured POC-normalized photosynthetic parameters to show that α^C and P_m^C can play a greater role than β^C in determining the competitive outcome between *P. antarctica* and *F. cylindrus* in both shallow and deep mixed-layer environments of the Ross Sea.

Key index words: **dynamic irradiance; *Fragilariopsis cylindrus; Phaeocystis antarctica;* photosynthesis; Southern Ocean**

Abbreviations: **DD, diadinoxanthin; DML, deep mixed layer; DT, diatoxanthin; E_k, photoacclimation index; EPC, excess photosynthetic capacity; F_v/F_m, maximum photosynthetic conversion efficiency of PSII; MML, medium mixed layer; *P–E*, photosynthesis versus irradiance; (P_m^*), maximum chl *a*–specific carbon fixation rates; SML, shallow mixed layer; α^*, initial slope of the *P–E* curve; β^*, photoinhibition parameter; Φ_m, quantum yield of photosynthesis**

The Southern Ocean is one of the world's three high-nutrient low-chl regions, where chl *a* concentrations are low relative to water-column macronutrient (nitrate and phosphate) concentrations. Despite this, phytoplankton concentrations are still relatively high compared to oligotrophic oceans, and thus, the Southern Ocean is important for the biological uptake and sequestration of atmospheric carbon dioxide (CO_2; Caldeira and Duffy 2000, Takahashi et al. 2002). Of the roughly 0.2 Gt of anthropogenic CO_2 taken up annually by the Southern Ocean, approximately half is mediated by the activity of phytoplankton (Takahashi et al. 2002, Roy et al. 2003, Gurney et al. 2004). The Ross Sea, one of the most productive Southern Ocean regions, accounts for almost 30% of annual primary production (Arrigo et al. 2008).

[1]Received 30 June 2009. Accepted 10 May 2010.
[2]Author for correspondence: e-mail mmmills@stanford.edu.

The annual cycle of phytoplankton biomass in the Ross Sea follows a predictable pattern (Arrigo et al. 1998b, Smith et al. 2003). In the austral fall and winter, biomass is at a minimum due to low incident irradiance and high sea-ice cover. Salination of surface waters during sea-ice formation drives deep convection that mixes nutrients up from below. As the sea-ice retreats, light becomes available within these nutrient-rich surface waters, resulting in intense spring phytoplankton blooms (Arrigo and Van Dijken 2004) with spatially distinct phytoplankton assemblages (Arrigo et al. 1999). In deeply mixed waters, such as in the Ross Sea polynya or early spring in Terra Nova Bay, the haptophyte *P. antarctica* dominates the spring phytoplankton bloom (Arrigo et al. 2000, Fonda Umani et al. 2002). In contrast, diatoms dominate shallower mixed layers located along the western continental shelf and along the ice edge in Terra Nova Bay (Arrigo et al. 2000). Hypotheses put forward to explain these distribution patterns include differences in vertical mixing regimes (Arrigo et al. 2003b), micronutrient distributions (Van Hilst and Smith 2002, Tagliabue and Arrigo 2005), variable grazing pressure (Van Hilst and Smith 2002), and/or seeding of the water column with ice algae as the ice edge retreats (Garrison et al. 1983, Schloss and Estrada 1994, Arrigo et al. 2003a). Arrigo et al. (2003b) used an ecosystem model of the Ross Sea to show that while the availability of the micronutrient Fe controls the productivity of these blooms, their taxonomic composition depends on the taxon-specific responses to mixed-layer irradiance. This result, however, has yet to be confirmed. A better understanding of how these phytoplankton acclimate to changes in water-column irradiance characteristics may help explain these distinct assemblages. In addition, because these taxa differ in their capacities for CO_2 fixation (Arrigo et al. 1999, 2002), determining the controls of phytoplankton species composition and productivity is critical to understanding the variability in Southern Ocean CO_2 uptake.

In a relatively turbulent upper mixed layer, irradiance can fluctuate from full sunlight to complete darkness over just a few hours (MacIntyre et al. 2000, Ross et al. 2008), and thus, phytoplankton must photoacclimate accordingly. Photoacclimation consists of a combination of physiological responses that maximize photosynthetic carbon assimilation while balancing the costs of prevention and repair of photodamage that results from the absorption of excess light energy by the photosynthetic apparatus. The degree of damage depends on the time and intensity of exposure. In the rapidly changing light environment characteristic of a turbulent mixed layer, phytoplankton cells move between light-limiting and light-saturating conditions and experience photoinhibitory damage when the capacity for photoprotection is exceeded.

Phytoplankton photoacclimation responses are highly time dependent, ranging from short-term xanthophyll cycling that operates on timescales of several seconds to minutes to long-term changes in photosynthetic unit (PSU) size or number that take place in a matter of hours to days (Marra 1978a,b, Cullen and Lewis 1988, Pahlwostl and Imboden 1990, Franks and Marra 1994, Geider et al. 1996, MacIntyre et al. 2000, Behrenfeld et al. 2002, Havelkova-Dousova et al. 2004, Lavaud et al. 2007). Under low irradiance, photoautotrophic cells maximize photon capture by increasing either PSU number or PSU size (Falkowski 1980, Falkowski and La Roche 1991, Moore et al. 2006), the former strategy being more common among eukaryotic phytoplankton (Falkowski 1980). PSU number and/or size decreases when phytoplankton are exposed to increasingly high irradiance.

One way of dealing with excess absorbed energy is through heat dissipation mediated by photoprotective xanthophyll-cycle pigments. A sudden increase in light results in rapid enzymatic de-epoxidation of the xanthophyll pigment diadinoxanthin (DD) to form the pigment diatoxanthin (DT). DT scavenges excess energy within the pigment bed and dissipates it as heat. The DD–DT interconversion is regulated within seconds to minutes of irradiance changes so that excess energy can be dissipated rapidly. Once the period of excess energy absorption ceases, DT is epoxidated back to DD. The rapid cycling of xanthophyll pigments quenches potentially harmful excess energy experienced by cells that are rapidly shifted to higher irradiance and partially explains why diatoms are adapted to light intensity fluctuations (Lavaud et al. 2004).

Different phytoplankton taxa likely have different abilities to acclimate to the changing light fields that characterize deeply and shallowly mixed water columns. The capacity for phytoplankton to increase rates of carbon fixation when exposed to high irradiance is known as excess photosynthetic capacity (EPC; Kana and Glibert 1987). EPC determines the ability of an alga to utilize fluctuating light (e.g., light in a turbulent mixed layer) and is used to segregate algae into ''layer formers,'' those that are adapted to relatively high and constant irradiance, and ''mixers,'' those that are adapted to lower and more variable irradiance (Cullen and MacIntyre 1998). Mixers are characterized by their high EPC, while layer formers have very limited EPC. In deeply mixed water columns, the flux of photons at the base of the mixed layer may be insufficient to drive electron turnover in each reaction center. Under these light-limiting conditions, EPC may result from an increased number of PSUs that allow for more electron turnover (Kana and Glibert 1987). Furthermore, when irradiance increases as phytoplankton are mixed toward the surface, EPC ensures that phytoplankton can utilize the greater flux of photons for photochemistry. Such a strategy is believed to maximize photosynthetic

rates in dynamic light regimes and may help explain the distinct spatial distributions observed for many phytoplankton taxa, including those in the Ross Sea.

The goal of the present study was to compare and contrast the photoacclimation strategies of two dominant Southern Ocean phytoplankton, the haptophyte *P. antarctica* and the diatom *F. cylindrus*, under dynamic irradiance intended to simulate the light field of rapidly mixing shallow and deep mixed layers (DMLs). Acclimation responses were characterized using photosynthesis versus irradiance (*P–E*) measurements, pigment concentration and composition, absorption spectra, PSII efficiency, and cellular carbon and nitrogen content. Finally, we used the data from these experiments to help explain the role of the mixed-layer light regime in controlling the distinct taxonomic distributions of phytoplankton observed in the Ross Sea.

MATERIALS AND METHODS

Two strains of the Antarctic phytoplankton *P. antarctica* (CCMP1374, CCMP1871) and one strain of *F. cylindrus* (CCMP1102) were obtained from the Center for Culture of Marine Phytoplankton (CCMP), Bigelow Laboratory for Ocean Science, West Boothbay Harbor, Maine, and grown in semicontinuous cultures (750 mL) in artificial seawater (Price et al. 1989) amended with f/2 medium (Guillard and Ryther 1962). The cultures were grown at 2°C under three different dynamic irradiance treatments that were chosen to simulate light levels characteristic of a range of mixed-layer depths observed in the Ross Sea, Antarctica. This was achieved using Sylvania DuLux L 55W (FT55DL/841) lamps (Sylvania, Danvers, MA, USA) with dimmable ballasts (Sylvania Quicktronic Pho-Dim) that were regulated via a Velleman K8000 computer interface board (Velleman Inc., Fort Worth, TX, USA). The three mixed-layer irradiances that we simulated included a DML (0–250 μmol quanta $\cdot$ $m^{-2} \cdot s^{-1}$, mean: 65 μmol quanta $\cdot$ $m^{-2} \cdot s^{-1}$), a moderately shallow mixed layer (MML, 25–250 μmol quanta $\cdot$ $m^{-2} \cdot s^{-1}$, mean: 125 μmol quanta $\cdot$ $m^{-2} \cdot s^{-1}$), and a very shallow mixed layer (SML, 25–550 μmol quanta $\cdot$ $m^{-2} \cdot s^{-1}$, mean 250 μmol quanta $\cdot$ $m^{-2} \cdot s^{-1}$). Irradiance in each treatment was measured using a Biospherical Instruments QSL Quantum Scalar Laboratory Sensor (Biospherical Instruments Inc., San Diego, CA, USA).

Briefly, the DML treatment was designed to simulate periods when the mixed-layer depth exceeds the euphotic depth, a situation that is not uncommon in the Ross Sea polynya (Arrigo et al. 1998a,b, 2000). The light period (from minimum to maximum and back to minimum) in the DML treatment lasted 1 h and was followed by 1 h of darkness. The MML irradiance treatment simulated conditions where the mixed-layer depth and the euphotic depth were approximately equal, while the SML dynamic light treatment approximated the shallowest mixed layers, such as those measured in Terra Nova Bay (Arrigo et al. 1999). We recognize that the understanding of how turbulence is transferred within a mixed layer is far from perfect, and thus, mixed-layer irradiance fields are poorly constrained. However, our intention was to simulate the irradiance range a cell might be exposed to in water columns with different mixing characteristics. In the SML, MML, and DML treatments, the complete light cycle lasted 2 h. A more detailed description of the dynamic irradiance treatments can be found in Kropuenske et al. (2009).

Cultures were grown for ~10 generations in semicontinuous culture to acclimate cells to the irradiance treatment. All cultures were grown until midexponential phase, determined by measuring in vivo fluorescence every other day, at which time 120 mL of culture was collected and sampled for the variables listed below. Cultures were optically thin at the time of sampling, with cell concentrations generally ranging $1–27 \times 10^9$, $5–25 \times 10^9$, and $1–15 \times 10^9$ cells $\cdot$ L^{-1} for *F. cylindrus* #1102, *P. antarctica* #1871, and *P. antarctica* #1374, respectively.

Physiological measurements included *P–E* curves using the ^{14}C-bicarbonate incorporation technique (Lewis and Smith 1983), the maximum photochemical conversion efficiency of PSII (F_v/F_m), xanthophyll pigment concentrations using HPLC, and cell abundance. The methods for the measurement of these parameters were recently described in Kropuenske et al. (2009), and we direct the reader there for a full description. We note that care was taken to freeze the pigment samples in liquid nitrogen immediately after filtration to ensure that the de-epoxidation state of the xanthophyll pool reflected in vivo conditions. HPLC pigment concentrations were not sampled from every culture, and thus, fluorometric chl *a* concentrations are used throughout the manuscript, except for the normalization of xanthophyll-cycle pigments.

In addition to the above parameters, we measured POC and particulate organic nitrogen (PON) concentrations, phytoplankton absorption spectra, and the quantum yield of photosynthesis (Φ_m) as described in our recently published companion paper Arrigo et al. (2010). EPC (Kana and Glibert 1987) was calculated as the ratio of the maximum POC-normalized photosynthetic rate (P^C_m) to the POC-normalized productivity at the mean irradiance (E_g) of the dynamic light treatment (P^C_{Eg}).

Statistical analyses were performed to assess within- and between-species treatment differences using two-factor analyses of variance and the Fisher protected least significant difference (PLSD) means comparison tests ($P < 0.05$).

RESULTS

Pigment, carbon, and nitrogen content. The cellular chl *a* content of *P. antarctica* #1374 and *F. cylindrus* #1102 generally decreased with increasing growth irradiance (Table 1). *P. antarctica* #1871 exhibited more variability than *F. cylindrus* #1102 or *P. antarctica* #1374, decreasing from the DML to the MML treatment, but then increasing from the MML to the SML treatment. In the high-light SML treatment, chl *a* per cell was reduced to ~0.04 and 0.15–0.18 pg $\cdot$ $cell^{-1}$ in *F. cylindrus* #1102 and *P. antarctica* (both strains), respectively.

Concentrations of the xanthophyll-cycle pigments DD and DT, normalized to chl *a* (mol $\cdot$ mol^{-1}) did not change with increasing growth irradiance in *P. antarctica* #1374, while *P. antarctica* #1871 showed an ~4-fold increase between the DML and SML dynamic light treatments (Table 1). Despite the large increase in DT concentration with growth irradiance in *P. antarctica* #1871, the de-epoxidation ratio (DT/[DD + DT]) changed very little with light treatment in both strains of *P. antarctica*. In contrast, xanthophyll-cycle pigment content in *F. cylindrus* #1102 responded much more strongly to growth irradiance than did *P. antarctica*, with DD decreasing by 70% and DT increasing by ~150% between the DML and SML treatments. As a result, the de-epoxidation ratio

TABLE 1. Chl *a* concentration, xanthophyll (DD and DT) content, and de-epoxidation ratio of *Fragilariopsis cylindrus*, *Phaeocystis antarctica* #1871, and *P. antarctica* #1374 grown under the three dynamic irradiance regimes.

	Chl *a* (pg · cell^{-1})	DD (mol · mol chl *a*$^{-1}$)	DT (mol · mol chl *a*$^{-1}$)	DT/[DD + DT]
F. cylindrus				
DML	0.16 (0.174)	0.21 (0.007)	0.13 (0.064)	0.35 (0.121)
MML	0.05 (0.063)	0.16 (0.020)	0.14 (0.072)	0.43 (0.184)
SML	0.04 (0.051)	0.14 (0.010)	0.95 (0.13)	0.87 (0.196)
P. antarctica #1871				
DML	0.15 (0.120)	0.02 (0.052)	0.02 (0.015)	0.14 (0.208)
MML	0.06 (0.052)	0.02 (0.051)	0.03 (0.030)	0.53 (0.545)
SML	0.15 (0.250)	0.07 (0.027)	0.08 (0.039)	0.55 (0.100)
P. antarctica #1374				
DML	0.31 (0.044)	0.06 (0.005)	0.05 (0.006)	0.51 (0.055)
MML	0.19 (0.095)	0.04 (0.009)	0.05 (0.007)	0.55 (0.131)
SML	0.18 (0.160)	0.05 (0.012)	0.04 (0.009)	0.42 (0.116)

Mean (±SD) are presented for at least three replicates. DD, diadinoxanthin; DML, deep mixed layer; DT, diatoxanthin; MML, medium mixed layer; SML, shallow mixed layer.

increased by more than a factor of two between the DML and SML treatments (Table 1). The bulk xanthophyll-cycle pigment concentrations presented in Table 1 were determined at randomly selected points during the light cycle of the dynamic light treatments. When we sampled at the maximum and the minimum points in the light cycle, DT/(DD + DT) in *F. cylindrus* #1102 varied significantly, increasing ~2-fold between the time of minimum and maximum irradiance (Fig. 1A). In contrast, the fraction of the xanthophyll-cycle pigment pool that was de-exposidated remained relatively constant over the light cycle for both strains of *P. antarctica* (Fig. 1, B and C).

The cellular C content of the three algae exhibited no clear trend with irradiance treatment (Table 2). In *F. cylindrus* #1102, C · cell^{-1} decreased 3-fold between the DML and MML treatment (from 10.2 to 3.17 pg C · cell^{-1}), but like chl *a* · cell^{-1}, there was no further decline between the MML and high-light SML treatment. In *P. antarctica* #1871, C · cell^{-1} also declined 3-fold from the DML to the MML treatment, but then increased in the SML treatment, similar to the behavior observed for chl *a* · cell^{-1}. *P. antarctica* #1374 exhibited yet a different pattern across light treatments, with the highest (SML) and the lowest (DML) light treatments having similar values (30–32 pg C · cell^{-1}) and the intermediate light level (MML) exhibiting the highest cellular C content. One clear generalization that can be made is that the cellular C content of *P. antarctica* was consistently higher than that of *F. cylindrus* #1102 in all irradiance treatments. There also was no particular trend observed between irradiance treatment and the POC:PON ratio for any of the algae examined here (Table 2). In general, POC:PON exhibited relatively little variation, either between irradiance treatments or between algal taxa, ranging from 5.8 to 7.4.

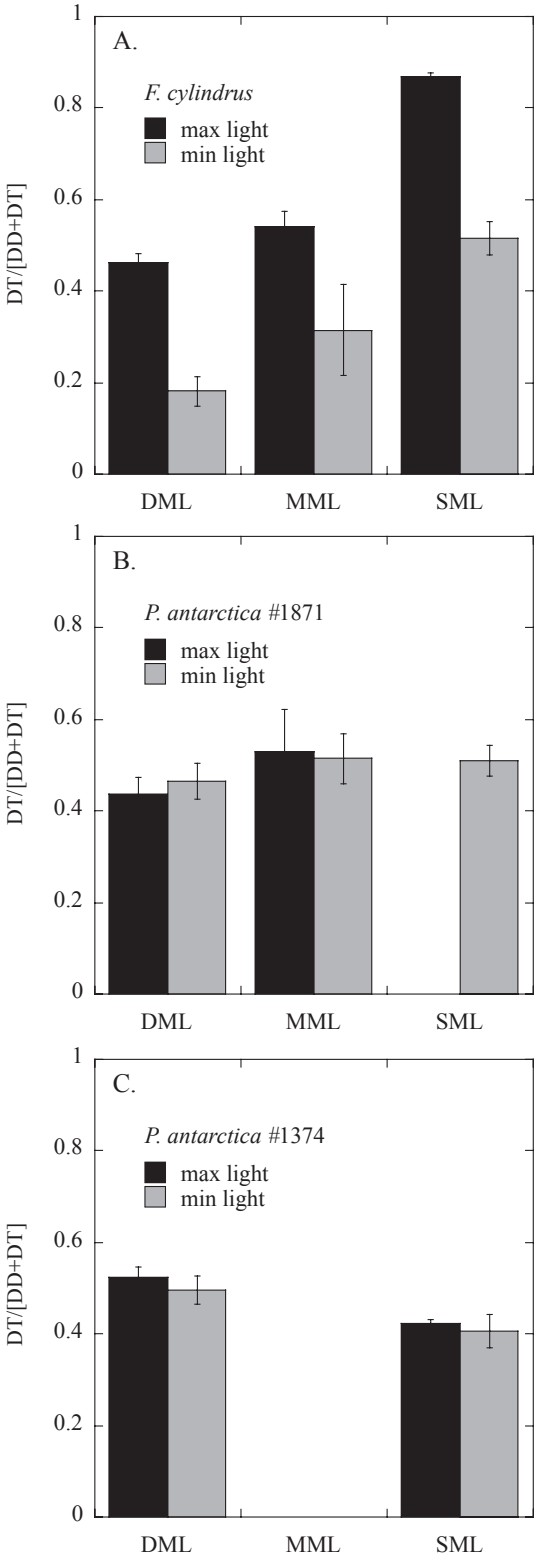

FIG. 1. Differences in the xanthophyll-cycle pigment de-epoxidation ratio (DT/[DD + DT]) for *Fragilariopsis cylindrus* #1102, *Phaeocystis antarctica* #1871, and *P. antarctica* #1374 at the maximum and minimum irradiance in the dynamic light treatments. DD, diadinoxanthin; DML, deep mixed layer; DT, diatoxanthin; MML, medium mixed layer; SML, shallow mixed layer.

The phytoplankton we studied exhibited markedly different responses in their C:chl *a* ratios as a function of dynamic irradiance treatment (Fig. 2). *F. cylindrus* #1102 maintained a relatively low but uniform C:chl *a* ratio that ranged only from 65 to 80 g C · g^{-1} chl *a* across the three dynamic irradiance treatments. In contrast, the C:chl *a* ratio of *P. antarctica* #1871 was ~230 g C · g^{-1} chl *a* in the DML treatment and decreased by ~33% at the higher average irradiance of the MML and SML treatments. Conversely, in *P. antarctica* #1374 the C:chl *a* ratio increased by >2-fold (from 100 to 230 g C · g^{-1} chl *a*) between the DML and the MML irradiance treatments, although it dropped slightly in the SML light treatment.

TABLE 2. Cellular C content, particulate organic carbon to nitrogen ratio (POC:PON), and F_v:F_m for cultures grown under simulated deep (DML), medium (MML), and shallow (SML) mixed-layer irradiance.

	pg C:cell	POC:PON	F_v/F_m
Fragilariopsis cylindrus			
DML	10.17 ± 0.56^{a}	6.2 ± 0.25^{a}	0.58 ± 0.020^{a}
MML	3.17 ± 0.16^{b}	5.8 ± 0.59^{a}	0.55 ± 0.043^{a}
SML	3.05 ± 2.57^{b} (a,a,a)	7.1 ± 0.16^{b} (a,a,a)	0.44 ± 0.012^{b} (a,ab,a)
Phaeocystis antarctica #1871			
DML	34.37 ± 0.95^{a}	7.1 ± 0.34^{a}	0.62 ± 0.018^{a}
MML	8.84 ± 0.24^{b}	7.4 ± 1.06^{a}	0.63 ± 0.031^{a}
SML	22.12 ± 3.81^{c} (b,b,b)	6.8 ± 0.15^{a} (b,a,a)	0.59 ± 0.006^{b} (a,b,b)
P. antarctica #1374			
DML	32.38 ± 1.02^{a}	6.8 ± 0.26^{a}	0.65 ± 0.023^{a}
MML	43.00 ± 3.03^{b}	7.3 ± 0.71^{a}	0.56 ± 0.013^{b}
SML	30.06 ± 1.90^{a} (b,c,c)	7.3 ± 0.32^{a} (b,b,a)	0.48 ± 0.037^{b} (a,a,a)

The superscripted letters represent between-treatment differences within species. The letters in parentheses distinguish between-species differences in the dynamic light treatments. Letters in parentheses are ordered DML, MML, SML and are compared between species vertically. Treatments or species not connected by the same letter are significantly different at the 0.05 alpha level.

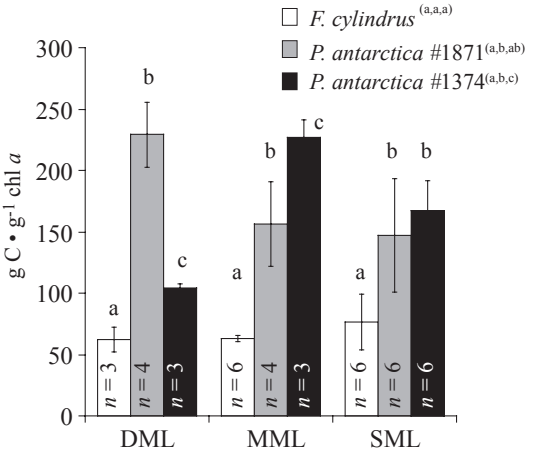

FIG. 2. Mean (±SD) C:chl *a* ratios of *Fragilariopsis cylindrus* #1102, *Phaeocystis antarctica* #1871, and *P. antarctica* #1374 sampled during midexponential growth in the DML, MML, and SML light treatments. Letters above each bar at each dynamic light treatment denote between-species differences. Subscripted letters in the legend denote within-species treatment differences. Subscripted letters are ordered as (DML, MML, and SML). Species or treatments not connected by the same letter are different at the 0.05 alpha level. DML, deep mixed layer; MML, medium mixed layer; SML, shallow mixed layer.

Photosynthetic characteristics. The maximum photochemical conversion efficiency of PSII (F_v/F_m) for all three of our phytoplankton cultures was within the range expected for healthy cells for the duration of the experiment (Table 2). The two general patterns that emerged were that F_v/F_m decreased slightly with increasing growth irradiance and that, on average, F_v/F_m was higher in the *P. antarctica* strains than in *F. cylindrus* #1102. There also was a noticeable difference in F_v/F_m as a function of irradiance between the two *P. antarctica* strains. F_v/F_m declined by 5% and 25% in *P. antarctica* #1871 and #1374, respectively, between the lowest and highest irradiance treatments.

The *P. antarctica* strains exhibited maximum chl *a*–specific carbon fixation rates (P^*_m) that were 2- to 8-fold higher than those measured for *F. cylindrus*, with larger differences generally at the lowest dynamic light treatments (Fig. 3A). While *F. cylindrus* #1102 exhibited no significant difference in P^*_m between the three dynamic light treatments (0.7–1.7 g C · g^{-1} chl *a* · h^{-1}), the P^*_m of *P. antarctica* declined with increasing irradiance treatment, although the two strains differed in their sensitivity to changes in light. For example, although P^*_m for *P. antarctica* #1871 dropped markedly as mean irradiance was increased from the DML (7.2 g C · g^{-1} chl *a* · h^{-1}) to the MML treatment (3.6 g C · g^{-1} chl *a* · h^{-1}), there was no additional change in P^*_m as light was increased further in the SML treatment. Conversely, the P^*_m for *P. antarctica* #1374 did not change significantly between the DML and MML dynamic irradiance treatment (8.4–8.7 g C · g^{-1} chl *a* · h^{-1}) but dropped substantially in the SML treatment (3.4 g C · g^{-1} chl *a* · h^{-1}).

The initial slope of the *P–E* curve (α*) in the DML and MML treatments was greatest for *P. antarctica* #1374, followed by *P. antarctica* #1871 and *F. cylindrus* #1102. In the SML treatment, α* was approximately the same for all three cultures (Fig. 3B). *P. antarctica* #1871 was the only one of the three strains to exhibit a progressive decrease in α* with increasing irradiance, falling from 0.08 to 0.05 g C · g^{-1} chl *a* · h^{-1} (μmol quanta · m^{-2} · s^{-1})$^{-1}$ between the DML and SML treatments. In *P. antarctica* #1374, α* actually increased by 24% between the DML and MML treatments, then dropped dramatically (by 62%) in the SML treatment. *F. cylindrus* #1102 showed no clear trend in α* as a function of light treatment, exhibiting the lowest values during the intermediate irradiance MML treatment.

The most dramatic photophysiological difference between taxa was observed for the photoinhibition

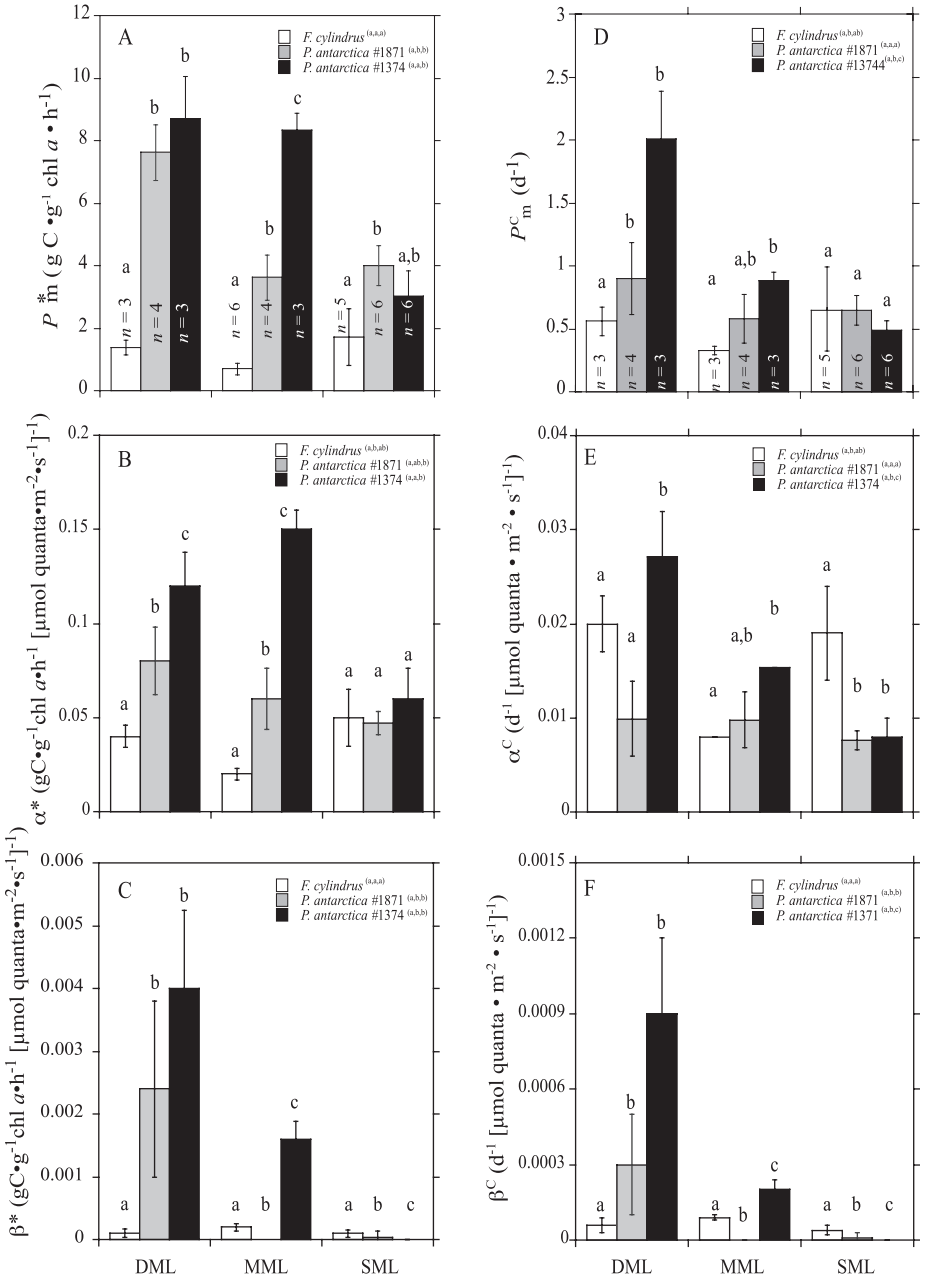

FIG. 3. Mean (±SD) photosynthesis versus irradiance (*P–E*) coefficients for *Fragilariopsis cylindrus* #1102, *Phaeocystis antarctica* #1871, and *P. antarctica* #1374 sampled during midexponential growth in the dynamic light treatments: (A) P^*_m (g C · g^{-1} chl *a* · h^{-1}), (B) α* (g C · g^{-1} chl *a* · h^{-1} [μmol quanta · m^{-2} · s^{-1}]$^{-1}$), (C) β* (g C · g^{-1} chl *a* · h^{-1} [μmol quanta · m^{-2} · s^{-1}]$^{-1}$), (D) P^C_m (d^{-1}), (E) α^C (d^{-1} [μmol quanta · m^{-2} · s^{-1}]$^{-1}$), (F) β^C (d^{-1} [μmol quanta · m^{-2} · s^{-1}]$^{-1}$). Statistical differences indicated as in Figure 2. DML, deep mixed layer; MML, medium mixed layer; SML, shallow mixed layer.

parameter (β*). In *F. cylindrus* #1102, β* was consistently very small ($1–2 \times 10^{-4}$ g C · g^{-1} chl *a* · h^{-1} [μmol quanta · m^{-2} · s^{-1}]$^{-1}$) and constant across the dynamic irradiance treatments (Fig. 3C), suggesting that little if any photoinhibition was taking place. In contrast, β* was much higher for both strains of *P. antarctica* in the DML treatment and decreased substantially as the treatment irradiance increased. Virtually no photoinhibition was measurable in *P. antarctica* #1871 and #1374 when grown at the MML and SML treatments. *F. cylindrus* #1102 had a 15- to 30-fold lower susceptibility to photoinhibition than both *P. antarctica* strains in the DML treatment and ~15-fold lower susceptibility than *P. antarctica* #1374 in the MML treatment.

The relative differences in photosynthetic parameters among the three phytoplankton groups generally decreased when carbon uptake was normalized by POC instead of chl *a* (Fig. 3, D–F). This is because of the large differences in the C:chl *a* ratios exhibited by these phytoplankton cultures in association with the various irradiance treatments. In the DML treatment, *P. antarctica* #1871 and #1374 had maximum POC-normalized photosynthetic rates (P^C_m) that were 1.5 and 3.5 times greater, respectively, than *F. cylindrus* #1102 (Fig. 3D). However, whereas P^C_m for *P. antarctica* #1374 decreased markedly at higher irradiance treatments, both *P. antarctica* #1871 and *F. cylindrus* #1102 exhibited no such decrease. Finally, no differences

in P_m^C were detected among the three taxa when grown under the SML irradiance treatment.

The trends in POC-normalized α^C and β^C were broadly similar to those observed for their chl *a*–normalized counterparts (Fig. 3, E and F), with a few exceptions. *P. antarctica* #1374 exhibited a greater relative decline in α^C with light treatment (Fig. 3E) than was observed for α^* (Fig. 3B). In the DML irradiance treatment, the α^C of *F. cylindrus* #1102 was 80% higher than that measured for *P. antarctica* #1871, while in the SML treatment, α^C for *F. cylindrus* #1102 was ~2.5-fold higher than for both *P. antarctica* strains.

The photoacclimation index (E_k) was relatively constant with light treatment in *F. cylindrus* #1102 and remained ~1.5- to 3-fold lower than the E_k measured for both strains of *P. antarctica* (Fig. 4). The small changes in E_k were consistent with the relatively small changes observed in both P_m^* and α^* for *F. cylindrus* #1102 across the three dynamic irradiance treatments. Irradiance-dependent changes in E_k for *P. antarctica* mirrored the pattern seen for chl $a \cdot \text{cell}^{-1}$. *P. antarctica* #1871 had a minimum E_k in the MML treatment, while the E_k of *P. antarctica* #1374 decreased as average irradiance increased, contrary to our expectations that E_k would rise with increasing mean irradiance.

The maximum quantum yield of photosynthesis (Φ_m) for *P. antarctica* #1374 was surprisingly high under both the DML and MML treatments, and not significantly different from the theoretical maximum of 0.125 mol C · mol^{-1} quanta (Table 3). This value was reduced somewhat in the SML treatment but was still very high at 0.09 mol C · mol^{-1} quanta. Similarly, *P. antarctica* #1871 also exhibited very high values for Φ_m at all three irradiance treatments, ranging from 0.09 to 0.10 mol C · mol^{-1} quanta and again approaching the theoretical maximum value. In contrast, the Φ_m for *F. cylindrus* #1102 was much lower, ranging from 0.02 to 0.06 mol C · mol^{-1} quanta, with the lowest value being observed in the MML irradiance treatment.

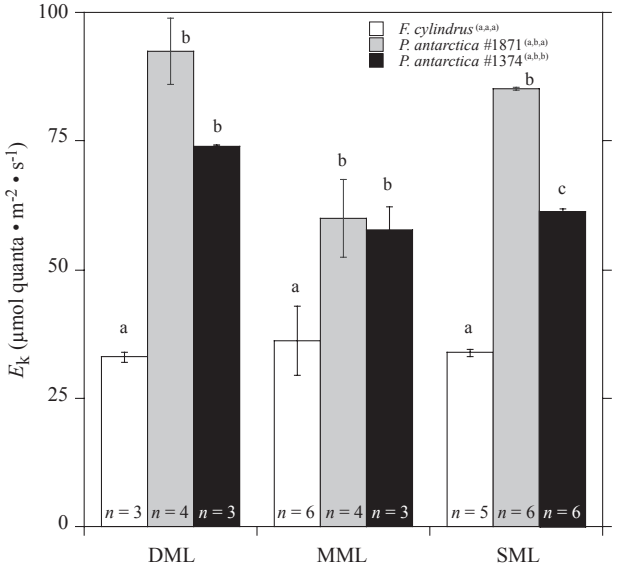

FIG. 4. Mean (±SD) photoacclimation index, E_k (µmol quanta · $\text{m}^{-2} \cdot \text{s}^{-1}$), for *Fragilariopsis cylindrus* #1102, *Phaeocystis antarctica* #1871, and *P. antarctica* #1374 sampled during midexponential growth in the three dynamic light treatments. Statistical differences indicated as in Figure 2. DML, deep mixed layer; MML, medium mixed layer; SML, shallow mixed layer.

Excess photosynthetic capacity was maximal for all three algae in the DML treatment (Fig. 5), with both strains of *P. antarctica* having the capacity to increase rates of photosynthesis by 3.5- to 4-fold relative to the rates measured at the average growth irradiance. This capacity was ~2-fold higher than that of *F. cylindrus* #1102. EPC in the MML treatment decreased to 1.3–1.5 for all three phytoplankton taxa, with no significant differences between the three phytoplankton detected. EPC was slightly lower still in the SML treatment, and again, no statistically significant differences were observed among the three phytoplankton. In addition, EPC in the SML treatment was not significantly different from unity for all three phytoplankton, indicating that none of the algae tested in this high dynamic irradiance treatment had EPC.

DISCUSSION

The photosynthetic parameters we present here are in good agreement with those measured for natural populations of *P. antarctica* (Palmisano et al. 1986, Saggiomo et al. 2002, Van Hilst and Smith 2002, Robinson et al. 2003). Field measurements of P_m^* range from 0.23 to 8.08 g C · g^{-1} chl $a \cdot \text{h}^{-1}$, consistent with our estimates of 3.42–8.35 g C · g^{-1} chl $a \cdot \text{h}^{-1}$. Similarly, our estimates of α^* (0.05–0.15 g C · g^{-1} chl $a \cdot \text{h}^{-1}$ [µmol quanta · $\text{m}^{-2} \cdot \text{s}^{-1}$]$^{-1}$) and E_k (60–90 µmol quanta · $\text{m}^{-2} \cdot \text{s}^{-1}$) are within the range of values measured for natural populations (0.01–0.18 g C · g^{-1} chl $a \cdot \text{h}^{-1}$ [µmol quanta · $\text{m}^{-2} \cdot \text{s}^{-1}$]$^{-1}$ and 2–144 µmol quanta · $\text{m}^{-2} \cdot \text{s}^{-1}$, respectively) (Palmisano et al. 1986, Saggiomo et al. 2002, Van Hilst and Smith 2002). Additionally, our estimates of Φ_m for *P. antarctica* are similar to those measured by Vaillancourt et al. (2003) in the Ross Sea polynya.

For *F. cylindrus*, our measurements of P_m^* and α^* (and thus E_k) also are consistent with those measured in diatom-dominated blooms in the Ross Sea (Saggiomo et al. 2002, Van Hilst and Smith 2002, Robinson et al. 2003), although our estimates of susceptibility to photoinhibition (β^*) are low relative to those of Van Hilst and Smith (2002). Saggiomo et al. (2002) measured P_m^* values of 1.86 g C · g^{-1} chl $a \cdot \text{h}^{-1}$ in waters of the western Ross Sea and the Terra Nova Bay polynya, which are typically dominated by diatom blooms, slightly greater than our highest P_m^* measurements for *F. cylindrus* #1102 grown in the SML treatment. However, the

TABLE 3. Summary of the mean (±SD) chl *a*, and carbon-normalized, coefficients from the *P–E* response curves, excess photosynthetic capacity (EPC), and quantum yield for the algae under the different dynamic light treatments.

	Dynamic light treatment	P^*_m	α^*	β^*	P^*_o	E_k	P^C_m	α^C	β^C	P^C_o	EPC $P^C_m:P^C_{Eg}$	Φ_m
Fragilariopsis cylindrus	DML	1.37 (0.231)	0.04 (0.006)	0.0001 (0.00007)	0.06 (0.016)	33.0 (0.098)	0.56 (0.113)	0.02 (0.003)	0.0001 (0.00003)	0.02 (0.007)	1.9 (0.03)	0.06 (0.011)
	MML	0.70 (0.188)	0.02 (0.003)	0.0002 (0.00006)	0.05 (0.020)	36.2 (6.78)	0.33 (0.031)	0.01 (0.000)	0.0001 (0.00001)	0.02 (0.002)	1.3 (0.04)	0.02 (0.005)
	SML	1.71 (0.908)	0.05 (0.02)	0.0001 (0.00006)	0.19 (0.089)	33.8 (0.60)	0.65 (0.344)	0.02 (0.005)	0.00004 (0.00002)	0.07 (0.034)	1.14 (0.53)	0.05 (0.010)
Phaeocystis antarctica #1871	DML	7.17 (0.949)	0.08 (0.018)	0.0024 (0.0014)	0.37 (0.055)	92.5 (6.57)	0.90 (0.287)	0.01 (0.004)	0.0003 (0.00020)	0.05 (0.021)	4.3 (0.36)	0.10 (0.009)
	MML	3.63 (0.726)	0.06 (0.016)	N/D	0.22 (0.080)	59.9 (7.64)	0.58 (0.196)	0.01 (0.003)	N/D	0.04 (0.017)	1.5 (0.10)	0.10 (0.015)
	SML	3.97 (0.719)	0.05 (0.006)	0.00004 (0.00009)	0.26 (0.040)	85.1 (0.23)	0.65 (0.117)	0.01 (0.001)	0.00001 (0.00002)	0.04 (0.007)	1.1 (0.22)	0.093 (0.017)
P. antarctica #1374	DML	8.70 (1.359)	0.12 (0.018)	0.0040 (0.00125)	0.55 (0.079)	74.1 (0.26)	2.01 (0.374)	0.03 (0.005)	0.0009 (0.00030)	0.13 (0.022)	3.5 (0.02)	0.14 (0.021)
	MML	8.35 (0.538)	0.15 (0.010)	0.0016 (0.00029)	0.70 (0.029)	57.7 (4.58)	0.88 (0.067)	0.02 (0.000)	0.0002 (0.00004)	0.07 (0.002)	1.5 (0.06)	0.14 (0.017)
	SML	3.42 (0.536)	0.06 (0.016)	N/D	0.30 (0.148)	61.3 (0.33)	0.49 (0.077)	0.01 0.002	N/D	0.04 (0.145)	1.1 (0.22)	0.09 (0.029)

N/D, not detected; DML, deep mixed layer; MML, medium mixed layer; SML, shallow mixed layer. P^*_o and P^C_o are CO_2-uptake rates or release at $E = 0$ μmol quanta · $m^{-2} \cdot s^{-1}$. Units: P^*_m (g C · g^{-1} chl *a* · h^{-1}), α^* (g C · g^{-1} chl *a* · h^{-1} [μmol quanta · $m^{-2} \cdot s^{-1}$]$^{-1}$), β^* (g C · g^{-1} chl *a* · h^{-1} [μmol quanta · $m^{-2} \cdot s^{-1}$]$^{-1}$), P^*_o (g C · g^{-1} chl *a* · h^{-1}), E_k (μmol quanta · $m^{-2} \cdot s^{-1}$), P^C_m (d^{-1}), α^C (d^{-1} [μEin · $m^{-2} \cdot s^{-1}$]$^{-1}$), β^C (d^{-1} [μEin · $m^{-2} \cdot s^{-1}$]$^{-1}$), P^C_o (d^{-1}), Φ_m (mol C · mol^{-1} quanta).

FIG. 5. Excess photochemical capacity (mean ± SD) for *Fragilariopsis cylindrus* #1102, *Phaeocystis antarctica* #1871, and *P. antarctica* #1374 sampled during midexponential growth in the three dynamic light treatments. Statistical differences indicated as in Figure 2. DML, deep mixed layer; EPC, excess photosynthetic capacity; MML, medium mixed layer; SML, shallow mixed layer.

corresponding α*, β*, and E_k ranges determined in Saggiomo et al. (2002) were all consistent with our *F. cylindrus* #1102 *P–E* measurements. These similarities suggest that our results obtained using laboratory cultures can be used to better understand the distinct in situ distributions of these two phytoplankton taxa in the Ross Sea.

The photosynthetic response of the two *P. antarctica* strains used here differed considerably at times under the different dynamic irradiance treatments. The greatest observed difference was the C:chl *a* ratio of *P. antarctica* #1871, which was ~2-fold higher than that measured in *P. antarctica* #1374 in the DML treatment. The result of this increased C:chl *a* ratio was generally lower C-normalized *P–E* parameters for *P. antarctica* #1871 compared with *P. antarctica* #1374 in this treatment. However, in both strains of *P. antarctica* the photophysiological parameters measured here trended in the same direction when compared to *F. cylindrus* #1102 in response to the different dynamic irradiance treatments (Figs. 2–5), with the exception of α^C and β in the DML and MML treatments, respectively. Intraspecific variability between these two strains was also observed under static irradiances ranging from 5 to 125 μmol photon · $m^{-2} \cdot d^{-1}$, with the greatest differences being recorded at the lowest irradiance level (Arrigo et al. 2010).

Taxon-specific photophysiological differences. Broadly speaking, *P. antarctica* and *F. cylindrus* appear to employ different strategies of photoacclimation. The strains of *P. antarctica* tested here adjusted their photosynthetic parameters to a much greater degree in response to changes in the light regime than did

the *F. cylindrus* strain. For example, in addition to larger variation with irradiance in the C-normalized maximum photosynthetic rate, the photoinhibition coefficient (β^C) varied by two orders of magnitude with irradiance in *P. antarctica*, while only changing by a factor of two in *F. cylindrus*. Likewise, the initial slope, α^C, of the *P–E* curve varied 2- to 6-fold more across light treatments in *P. antarctica* than in *F. cylindrus*.

The highest rates of carbon uptake in both *P. antarctica* strains were observed in the DML irradiance treatment, the only treatment with a dark period. This finding suggests that the dark period is important to photosynthesis and growth for this species, consistent with the conclusion of Mortain-Bertrand (1989) who found that Antarctic phytoplankton are adapted to alternating low- and high-light intensities. In contrast, little difference in the rate of carbon fixation was detected for *F. cylindrus* #1102 between the DML and SML treatments, contrary to results presented in Mortain-Bertrand (1989), where four species of Antarctic diatoms exhibited higher rates of carbon fixation when grown under a 2:2 light:dark (L:D) cycle than when grown under either continuous light or a longer 12:12 L:D cycle.

The dark period in the DML treatment was intended to simulate mixing below the euphotic zone, a common phenomenon in the DMLs of the Ross Sea (Arrigo et al. 1998a,b, 2000). Transient darkness may provide a period for repair of photosystems that are likely to be photodamaged at the highest irradiance portion of in the dynamic irradiance cycle (Alderkamp et al. 2010). Photoinhibition (β*, Fig. 3C) develops from the damage to the D1 protein in the photosynthetic reaction centers of PSII under high irradiance (Marshall et al. 2000) and is manifested when the rate of D1 damage is greater than the photosystem repair rate (Baroli and Melis 1996). The dark period provides time for photosystem repair without having to deal simultaneously with photodamage. This repair period presumably maximizes the number of functional photosynthetic reaction centers available during the light period, resulting in higher P^*_m, α*, and Φ_m, but also higher β*. A related study, in which *P. antarctica* #1841 was grown under DML conditions and treated with lincomycin to inhibit repair of damaged D1 protein, provides strong evidence for this (Kropuenske et al. 2009). Comparison of control and repair-inhibited cultures after one 2 h L:D cycle revealed a >10% reduction in P^*_m, a >40% lower α*, and a >300% increase in β* in the lincomycin-treated cultures, highlighting the importance of repair mechanisms in maintaining photosynthetic performance in *P. antarctica*. However, photoinhibition (both β* and β^C) was at most 3% of the light-limited slope (α* and α^C) across all dynamic light treatments and doubtfully contributed to significant decreases in the fixation of C for any of the algae tested here.

Consistent with relatively higher β* in both strains of *P. antarctica* in the DML treatment, and with the low β* of *F. cylindrus* #1102 across dynamic light treatments, the cellular xanthophyll-cycle pigment content of both *P. antarctica* strains was less than that of *F. cylindrus*. The dissipation of light energy as heat occurs via the conversion of xanthophyll-cycle pigments from an epoxidized to a heat-dissipating de-expoxidized form and is one of the most important mechanisms of photoprotection for phytoplankton. All algae tested here contained the xanthophyll-cycle pigments DD and its de-epoxidated counterpart DT (Table 1). Our data show that *F. cylindrus* #1102 had a greater concentration of DT relative to chl *a* than both *P. antarctica* strains (Table 1) in all dynamic irradiance treatments, particularly the SML treatment.

The proportion of the xanthophyll-cycle pigment pool that was de-epoxidated was ~50% for both strains of *P. antarctica*, regardless of light treatment or the time of sampling during the light cycle. In contrast, the DT pool size of *F. cylindrus* #1102 cultures increased proportionally with increasing mean irradiance, with just 35% of its xanthophyll-cycle pigment pool as DT in the DML irradiance treatment and ~87% in the SML irradiance treatment. In two other species of diatoms (*Thalassiosira weissflogii* and *Chaetoceros brevis*) and the haptophyte *Emiliania huxleyi*, a higher ratio of photoprotective to photosynthetic pigments was found to be indicative of a higher tolerance to excessive irradiance (Van de Poll et al. 2006, 2007). Close to 100% of the cells measured in those studies with ratios <0.1 were nonviable after short-term exposure to high levels of irradiance. Additionally, the haptophyte *E. huxleyi* had a lower ratio of photoprotective to photosynthetic pigments and was more sensitive to excessive irradiance than *T. weissflogii* (Van de Poll et al. 2007). Thus, the high cellular concentrations of xanthophyll-cycle pigments in *F. cylindrus* #1102 suggest that it is better able to quench excess light energy through heat dissipation, allowing *F. cylindrus* #1102 to maintain its photosynthetic capacity by preventing or minimizing photoinhibitory damage at higher light levels. This interpretation is consistent with higher levels of nonphotochemical quenching and lower levels of photoinhibition that were observed in *F. cylindrus* #1102 compared with *P. antarctica* #1841 cultures measured in these same irradiance treatments (Kropuenske et al. 2009).

The reliance on xanthophyll cycling by *F. cylindrus* #1102 is evident not only from the significant differences observed in the degree of xanthophyll-cycle pigment de-epoxidation between irradiance treatments but also from variation in de-epoxidation between the minimum and maximum irradiance within each dynamic irradiance treatment. This reliance on within-treatment cycling between DT and DD was not observed for either strain of *P. antarctica* in any of the light treatments used here

and is consistent with the conclusion of Kropuenske et al. (2009) that while *P. antarctica* does utilize the xanthophyll cycle to dissipate excess energy, it is less dependent on this form of photoprotection than *F. cylindrus*. The lack of within-treatment differences in de-epoxidation ratio observed for *P. antarctica* is at odds with findings reported in Van Leeuwe and Stefels (2007) who observed higher ratios of DT:DD at the maximum irradiance, and lower ratios at the minimum irradiance, of a dynamic light cycle for *P. antarctica* #1871.

The lower xanthophyll-cycle pigment concentrations of *P. antarctica* corresponded with greater variability in photosynthetic parameters among irradiance treatments. These findings support the results of Kropuenske et al. (2009) who used measurements of nonphotochemical quenching, xanthophyll-cycle inhibition, and protein repair inhibition to show that *F. cylindrus* #1102 prioritizes photoprotection over rapid growth, while *P. antarctica* maximizes growth and must continuously repair photodamage. These results are also consistent with the findings of our companion paper (Kropuenske et al. 2010), which concludes that *F. cylindrus* #1102 relies upon extenstive xanthophyll-cycle activity as a way of reducing σPSII and tolerating high irradiance. In addition, our finding that *P. antarctica* adjusts its photosynthetic parameters to a larger degree than *F. cylindrus* #1102 supports another conclusion of Kropuenske et al. (2010) that *P. antarctica* acclimates to changing irradiance via changes in both photosynthetic capacity (PSU · cell^{-1} and $1/\tau$) and effective PSU size, leaving it more vulnerable to photoinhibition but explaining higher light-limited (α^*) and light-saturated (P_m^*) photosynthetic rates under DML and SML conditions (Fig. 3).

The irradiance in our experiments continually varied from limiting to saturating for the three algae over a 2 h period. However, only for *F. cylindrus* #1102 was the mean irradiance in all three dynamic light treatments saturating ($E_k <$ mean E_g), making a pigment pool proportionally high in photoprotective pigments beneficial. In contrast, the mean irradiance was greater than E_k in only the MML and SML treatments for both strains of *P. antarctica*. The lack of increase in photoprotective pigments by *P. antarctica* #1374 with rising dynamic irradiance, and relatively small increase observed in *P. antarctica* #1871 compared with *F. cylindrus* #1102 grown under the same conditions, coupled with limited de-epoxidation ratios in both strains, may have contributed to the precipitous decline in P_m^* and P_m^C between the DML treatment and the two higher dynamic light treatments. The only difference between the DML and MML treatments was the 1 h dark period, which appears crucial for *P. antarctica* #1871 to maintain very high photosynthetic rates. The steepest decline in P_m^* and P_m^C in *P. antarctica* #1374 occurred between MML and SML treatments, which differed only in their maximum irradiance exposure. These trends highlight the sensitivity of both *P. antarctica* strains to increasing irradiance intensity, particularly when a recovery period is not provided. This increased vulnerability could result in *P. antarctica* being unable to compete with other phytoplankton (e.g., diatoms) in high-light environments if sufficient dark periods for repair are not available.

Species distributions in the Ross Sea. The distribution of the dominant phytoplankton taxa in the Ross Sea is spatially distinct, with the colonial haptophyte *P. antarctica* typically dominating water columns characterized by DMLs, such as the Ross Sea polynya, and diatoms dominating shallow mixed environments such as the marginal ice zone and Terra Nova Bay (Arrigo et al. 1999, 2002). The reason behind these observed distributions has proved difficult to discern. Previous studies documented that rates of primary productivity can be similar in blooms of these different taxa (Arrigo et al. 1999, Van Hilst and Smith 2002), despite their growing under different mixed-layer irradiance environments. Furthermore, photophysiological measurements made on natural populations failed to discern significant differences in either P_m^* or α^* for samples dominated by diatoms or by *P. antarctica* (Van Hilst and Smith 2002, Robinson et al. 2003).

Our dynamic irradiance treatments were intended to simulate both the deep and shallow mixed-layer depths characteristic of the central Ross Sea polynya and the western Ross Sea (including Terra Nova Bay), respectively. Unlike measurements made on mixed natural populations, our results using pure *F. cylindrus* and *P. antarctica* cultures demonstrate that these two algae exhibit significant differences in their photophysiological responses to different simulated mixed-layer irradiances. Moreover, these photophysiological differences provide a possible explanation for the spatial segregation of these taxa observed in the Ross Sea.

Under the two lower average mixed-layer irradiance treatments (DML and MML), the two *P. antarctica* strains fixed five to eight times more carbon than *F. cylindrus* #1102 per unit chl *a* and two to four times more per unit C. Additionally, both the photosynthetic efficiency under light limitation (α^* and α^C) and EPC were higher for the *P. antarctica* strains under these two irradiance treatments, giving them a distinct competitive advantage in the DMLs of the Ross Sea polynya where *P. antarctica* dominates. In deeply mixed water columns, *F. cylindrus* #1102 exhibited a 3-fold lower E_k than that observed in the *P. antarctica* strains, suggesting that it spends a greater proportion of the light cycle growing at maximum rates than the *P. antarctica* strains. The much higher growth rates of *P. antarctica* #1871 and #1374 offset any advantage that *F. cylindrus* #1102 may gain from attaining maximum productivity at a lower irradiance.

In contrast, at the higher light levels characteristic of SML, the difference in carbon fixation between these two taxa was dramatically reduced, particularly when expressed per unit C. Moreover, *F. cylindrus* #1102 had a 2.5-fold higher α^C and a 2- to 3-fold lower E_k than both *P. antarctica* strains in the SML treatment and, therefore, achieves maximum growth rates at lower irradiance and spends more time in the light cycle growing at its maximum rate. These data suggest that the relatively high potential P_m^C of the *P. antarctica* strains (which exhibited little taxonomic difference in P_m^C) gives them a competitive advantage in DMLs, while the relatively high α^C of *F. cylindrus* #1102 is advantageous in shallowly mixed environments. Using the designations defined by Cullen and MacIntyre (1998), our results suggest that *P. antarctica* is better adapted to a mixed water column (e.g., a mixer) and *F. cylindrus* #1102 is better adapted to a stratified water column (e.g., a layer former).

The difference between the chl *a*–based and C-based *P–E* coefficients highlights the importance of the rate-normalizing biomass parameter (MacIntyre et al. 2002). Photosynthetic rates per unit chl *a* do not necessarily equate with growth rate because of variations in cellular chl *a* content with light level. As light levels change, chl *a* will change as a proportion of total cell mass. C per cell may change as well, but generally not as much as chl *a*. For example, *P. antarctica* invests a relatively greater proportion of its fixed C into cellular growth at lower light than it does at higher mean irradiance. This phenomenon is likely because at high light, much of the carbon fixed by *P. antarctica* is shunted into the mucilaginous colony matrix (Schoemann et al. 2005). Rates of photosynthesis normalized to chl *a* concentration do not account for this change.

To further verify that the photophysiological differences we measured between *F. cylindrus* #1102 and the two *P. antarctica* strains are sufficient to explain distributions of these taxa in the Ross Sea, we performed a series of calculations using our experimentally derived *P–E* parameters to describe the growth of both strains of *P. antarctica* and of *F. cylindrus* #1102 under conditions of either shallow (7 m) or deep (50 m) mixing (Fig. 6). Surface irradiance (E_i) was calculated as described in Arrigo et al. (2008) and propagated through the water column as

$$E_z = E_i \cdot e^{(-0.04-0.05\ \mathrm{chl}\ a^{0.681})z} \quad (1)$$

where E_z is the irradiance at depth z, and chl *a* is the mean chl *a* concentration within the mixed layer ($mg \cdot m^{-3}$). Surface concentrations of diatoms and *P. antarctica* in the Ross Sea and the Terra Nova Bay polynyas were obtained from Arrigo et al. (2003b). For simplicity, chl *a* concentration in the mixed layer was held constant through time; this assumption had no impact on the relative difference in growth rate calculated for each alga. The C-normalized *P–E* parameters (Table 3) were used to calculate the mean C-specific growth rate for each algal taxa within the mixed layer at 1 m resolution. Parameters obtained from the SML and DML treatments were used to calculate growth rates in the 7 and 50 m mixed layers, respectively.

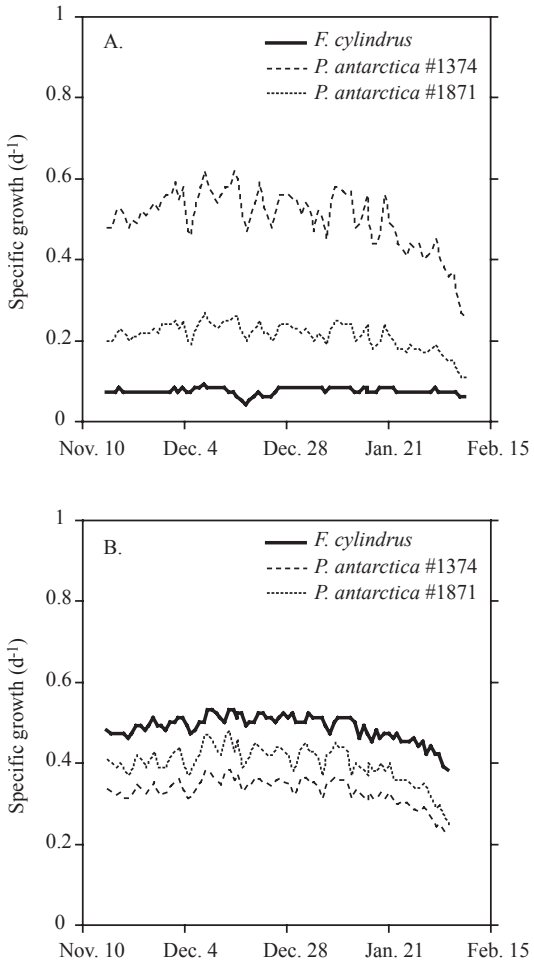

FIG. 6. Modeled mean specific growth of the *Fragilariopsis cylindrus* #1102 and *Phaeocystis antarctica* strains used here in a (A) 50 m mixed layer and (B) 7 m mixed layer.

In the 50 m mixed-layer calculation, the specific growth rate of *P. antarctica* #1374 during the spring bloom was on average ~7-fold higher throughout the mixed layer than that of *F. cylindrus* #1102 (Fig. 6A). The specific growth rate of *P. antarctica* #1374 was also 2.3-fold greater than that of *P. antarctica* #1871. These growth rate differences are attributable to the higher P_m^C and α^C of *P. antarctica* #1374 under deep mixing conditions (Fig. 3, D and E). Additionally, *P. antarctica* #1871 had a 3-fold higher specific growth rate than *F. cylindrus* #1102. In the 7 m mixed-layer calculation, the reverse was observed, with growth of *F. cylindrus* #1102 being ~1.5- and 1.2-fold higher than that of *P. antarctica* #1374 and #1871, respectively (Fig. 6B). Here, the

higher growth rate of *F. cylindrus* #1102 was due to its higher α^C under shallow mixing conditions (Fig. 3E), despite having a P_m^C that was not significantly different from that of *P. antarctica*.

In the 7 m mixed-layer simulation, between-taxa growth rate differences were reduced, suggesting that *F. cylindrus* #1102 would not dominate SMLs to the same degree that *P. antarctica* would dominate DMLs. This conclusion is consistent with field observations of the relative proportion of these two taxa in the Ross Sea. In the SMLs of the western shelf and Terra Nova Bay, diatoms dominate the bloom but generally account for only 70%–80% of the phytoplankton biomass, with *P. antarctica* accounting for most of the remaining 20%–30% (Arrigo et al. 1999). In contrast, the DMLs of the Ross Sea polynya are typically composed of >95% *P. antarctica*, with few diatoms present. Although diatoms generally have higher biomass than single-celled *P. antarctica*, colonial *P. antarctica* is far larger and has equal or greater biomass than many diatom species (Riegger and Robinson 1997). Thus, the fact that *P. antarctica* exhibits growth rates that are so much higher than *F. cylindrus* #1102 in the 50 m mixed layer may allow it to more completely dominate both phytoplankton abundance and biomass in Ross Sea polynya blooms.

It is important to note that our experiments were conducted with one strain of one diatom species and two strains of *P. antarctica*. In fact, the differences between the two *P. antarctica* strains were at times as great as that observed between *P. antarctica* and *F. cylindrus* #1102 (Figs. 2 and 3). Thus, any species distributions resulting from competition between these two taxa for growth-limiting resources likely rely on which strain of *P. antarctica* is present and if diatoms other than *F. cylindrus* are present. Despite the within-taxa variation observed for *P. antarctica*, the modeled growth rates suggest that *F. cylindrus* #1102 would dominate over either *P. antarctica* strain in a SML, while both strains of *P. antarctica* would dominate deeply mixed water columns, as is observed in the Terra Nova Bay and Ross Sea polynyas.

The important role of α^C in contributing to the dominance of *F. cylindrus* #1102 in a shallow mixed-layer environment runs counter to the hypothesis of Arrigo et al. (2003b) who suggested that photoinhibition of *P. antarctica* at high light was likely the dominant factor resulting in diatom dominance of shallow mixed-layer communities. Our study showed that both *P. antarctica* and *F. cylindrus* #1102 exhibited only slight or no photoinhibition in the SML treatment. However, both *P. antarctica* strains exhibited significantly reduced P_m at SML compared to DML conditions, suggesting a decline in photosynthetic capacity with increasing irradiance. Likewise, in a companion study, we found little difference in β^C between either *P. antarctica* strain and *F. cylindrus* #1102 grown under static irradiance conditions (Arrigo et al. 2010). Therefore, it appears now that the efficiency and maximum rate of photosynthesis play a greater role than photoinhibition in determining the competitive outcome between *P. antarctica* and *F. cylindrus* #1102 in shallow and deep mixed-layer environments.

These data clearly show that differences in the photosynthetic responses of *P. antarctica* and *F. cylindrus* #1102 to different simulated mixed-layer irradiance may significantly impact the phytoplankton distributions in the Ross Sea. Our conclusions contrast with those of Van Hilst and Smith (2002) who proposed that differences in photosynthetic responses between diatoms and *P. antarctica* were too small to explain the spatial distributions observed in the Ross Sea. They speculated that spatial and temporal variations in micronutrient distributions, vertical mixing regime, or variable grazing pressures contributed to the spatial distributions of phytoplankton observed in the Ross Sea. We caution that our results are for one diatom species and two strains of *P. antarctica* that responded somewhat differently to the mixed-layer irradiance treatments used here. Investigations of more diatom species and *P. antarctica* strains are thus warranted to verify these conclusions. Nonetheless, our work identifies the irradiance within a vertically mixed water column as a major forcing factor for distributions of phytoplankton in the Ross Sea.

We thank C. P. Chamberlain and the Stable Isotope Laboratory at Stanford University for providing space and machine time for the elemental analyses. This research was funded by the Ocean Carbon Sequestration Research Program, Biological and Environmental Research (BER), U.S. Department of Energy (grant #DE-FG02-04ER63891 and grant #DE-FG02-04ER63861).

Alderkamp, A. C., de Baar, H. J. W., Visser, R. J. W. & Arrigo, K. R. 2010. Can photoinhibition control phytoplankton abundance in deeply mixed water columns of the Southern Ocean? *Limnol. Oceanogr.* 55:1248–64.

Arrigo, K. R., DiTullio, G. R., Dunbar, R. B., Robinson, D. H., VanWoert, M., Worthen, D. L. & Lizotte, M. P. 2000. Phytoplankton taxonomic variability in nutrient utilization and primary production in the Ross Sea. *J. Geophys. Res. Oceans* 105:8827–45.

Arrigo, K. R., Dunbar, R. B., Lizotte, M. P. & Robinson, D. H. 2002. Taxon-specific differences in C/P and N/P drawdown for phytoplankton in the Ross Sea, Antarctica. *Geophys. Res. Lett.* 29:1938, doi: 10.1029/2002GL015277.

Arrigo, K. R., Mills, M. M., Kropuenske, L. R., Van Dijken, G. L., Alderkamp, A.-C. & Robinson, D. H. 2010. Photophysiology in two major Southern Ocean phytoplankton taxa: photosynthesis and growth of *Phaeocystis antarctica* and *Fragilariopsis cylindrus* under different irradiance levels. *Integr. Comp. Biol.* doi: 10.1093/icb/icq021.

Arrigo, K. R., Robinson, D. H., Dunbar, R. B., Leventer, A. R. & Lizotte, M. P. 2003a. Physical control of chlorophyll a, POC, and TPN distributions in the pack ice of the Ross Sea, Antarctica. *J. Geophys. Res. Oceans* 108:14.1–23.

Arrigo, K. R., Robinson, D. H., Worthen, D. L., Dunbar, R. B., DiTullio, G. R., VanWoert, M. & Lizotte, M. P. 1999. Phytoplankton community structure and the drawdown of nutrients and CO_2 in the Southern Ocean. *Science* 283:365–7.

Arrigo, K. R., Robinson, D. H., Worthen, D. L., Schieber, B. & Lizotte, M. P. 1998a. Bio-optical properties of the southwestern Ross Sea. *J. Geophys. Res. Oceans* 103:21683–95.

Arrigo, K. R. & Van Dijken, G. L. 2004. Annual changes in sea-ice, chlorophyll a, and primary production in the Ross Sea, Antarctica. *Deep-Sea Res. Part II Top. Stud. Oceanogr.* 51:117–38.

Arrigo, K. R., Van Dijken, G. L. & Bushinsky, S. 2008. Primary production in the Southern Ocean, 1997–2006. *J. Geophys. Res. Oceans* 113:C08004, doi:10.1029/2007JC004551.

Arrigo, K. R., Weiss, A. M. & Smith, W. O. 1998b. Physical forcing of phytoplankton dynamics in the southwestern Ross Sea. *J. Geophys. Res. Oceans* 103:1007–21.

Arrigo, K. R., Worthen, D. L. & Robinson, D. H. 2003b. A coupled ocean-ecosystem model of the Ross Sea: 2. Iron regulation of phytoplankton taxonomic variability and primary production. *J. Geophys. Res. Oceans* 108: No. C7, 3231, doi:10.1029/2001JC000856.

Baroli, I. & Melis, A. 1996. Photoinhibition and repair in *Dunaliella salina* acclimated to different growth irradiances. *Planta* 198:640–6.

Behrenfeld, M. J., Maranon, E., Siegel, D. A. & Hooker, S. B. 2002. Photoacclimation and nutrient-based model of light-saturated photosynthesis for quantifying oceanic primary production. *Mar. Ecol. Prog. Ser.* 228:103–17.

Caldeira, K. & Duffy, P. B. 2000. The role of the Southern Ocean in uptake and storage of anthropogenic carbon dioxide. *Science* 287:620–2.

Cullen, J. J. & Lewis, M. R. 1988. The kinetics of algal photoadaptation in the context of vertical mixing. *J. Plankton Res.* 10:1039–63.

Cullen, J. J. & MacIntyre, J. G. 1998. Behavior, physiology and the niche of depth-regulating phytoplankton. *In*: Anderson, D. M., Cembella, A. D. & Hallegraeff, G. M. [Eds.] *Physiological Ecology of Harmful Algal Blooms.* Springer-Verlag, Berlin, pp. 1–21.

Falkowski, P. G. 1980. Light-shade adaptation in marine phytoplankton. *In* Falkowski, P. G. [Ed.] *Primary Productivity in the Sea.* Plenum Press, New York, pp. 99–119.

Falkowski, P. G. & La Roche, J. 1991. Acclimation to spectral irradiance in algae. *J. Phycol.* 27:8–14.

Fonda Umani, S., Accornero, A., Budillon, G., Capello, M., Tucci, S., Cabrini, M., Del Negro, P., Monti, M. & De Vittor, C. 2002. Particulate matter and plankton dynamics in the Ross Sea Polynya of Terra Nova Bay during the austral summer 1997/98. *J. Mar. Syst.* 36:29–49.

Franks, P. J. S. & Marra, J. 1994. A simple new formulation for phytoplankton photoresponse and an application in a wind-driven mixed-layer model. *Mar. Ecol. Prog. Ser.* 111:143–53.

Garrison, D. L., Ackley, S. F. & Buck, K. R. 1983. A physical mechanism for establishing algal populations in frazil ice. *Nature* 306:363–5.

Geider, R. J., MacIntyre, H. L. & Kana, T. M. 1996. A dynamic model of photoadaptation in phytoplankton. *Limnol. Oceanogr.* 41:1–15.

Guillard, R. R. L. & Ryther, J. H. 1962. Studies of marine planktonic diatoms. I. *Cyclotella nana* Hustedt, and *Detonula confervacea* (Cleve) Gran. *Can. J. Microbiol.* 8:229–39.

Gurney, K. R., Law, R. M., Denning, A. S., Rayner, P. J., Pak, B. C., Baker, D., Bousquet, P., et al. 2004. Transcom 3 inversion intercomparison: model mean results for the estimation of seasonal carbon sources and sinks. *Glob. Biogeochem. Cycles* 18:GB1010, doi: 10.29/2003GB002111.

Havelkova-Dousova, H., Prasil, O. & Behrenfeld, M. J. 2004. Photoacclimation of *Dunaliella tertiolecta* (Chlorophyceae) under fluctuating irradiance. *Photosynthetica* 42:273–81.

Kana, T. M. & Glibert, P. M. 1987. Effect of irradiances up to 2000 μE $m^{-2}s^{-1}$ on marine *Synechococcus* WH7803—I. Growth, pigmentation, and cell composition. *Deep-Sea Res.* 34:479–95.

Kropuenske, L. R., Mills, M. M., Van Dijken, G. L., Alderkamp, A.-C., Berg, G. M., Robinson, D. H., Welschmeyer, N. A. & Arrigo, K. R. 2010. Strategies and rates of photoacclimation in two major Southern Ocean phytoplankton taxa: *Phaeocystis antarctica* (Haptophyta) and *Fragilariopsis cylindrus* (Bacillariophyceae). *J. Phycol.* 46, DOI: 10.1111/j.1529-8817.2010.00922.x

Kropuenske, L. R., Mills, M. M., Van Dijken, G. L., Bailey, S., Robinson, D. H., Welschmeyer, N. A. & Arrigo, K. R. 2009. Photophysiology in two major Southern Ocean phytoplankton taxa: photoprotection in *Phaeocystis antarctica* and *Fragilariopsis cylindrus. Limnol. Oceanogr. Methods* 54:1176–96.

Lavaud, J., Rousseau, B. & Etienne, A. L. 2004. General features of photoprotection by energy dissipation in planktonic diatoms (Bacillariophyceae). *J. Phycol.* 40:130–7.

Lavaud, J., Strzepek, R. F. & Kroth, P. G. 2007. Photoprotection capacity differs among diatoms: possible consequences on the spatial distribution of diatoms related to fluctuations in the underwater light climate. *Limnol. Oceanogr.* 52:1188–94.

Lewis, M. R. & Smith, J. C. 1983. A small volume, short-incubation-time method for measurement of photosynthesis as a function of incident irradiance. *Mar. Ecol. Prog. Ser.* 13:99–102.

MacIntyre, H. L., Kana, T. M., Anning, T. & Geider, R. J. 2002. Photoacclimation of photosynthesis irradiance response curves and photosynthetic pigments in microalgae and cyanobacteria. *J. Phycol.* 38:17–38.

MacIntyre, H. L., Kana, T. M. & Geider, R. J. 2000. The effect of water motion on short-term rates of photosynthesis by marine phytoplankton. *Trends Plant Sci.* 5:12–7.

Marra, J. 1978a. Effect of short-term variations in light-intensity on photosynthesis of a marine phytoplankter – laboratory simulation study. *Mar. Biol.* 46:191–202.

Marra, J. 1978b. Phytoplankton photosynthetic response to vertical movement in a mixed layer. *Mar. Biol.* 46:203–8.

Marshall, H. L., Geider, R. J. & Flynn, K. J. 2000. A mechanistic model of photoinhibition. *New Phytol.* 145:347–59.

Moore, C. M., Suggett, D. J., Hickman, A. E., Kim, Y. N., Tweddle, J. F., Sharples, J., Geider, R. J. & Holligan, P. M. 2006. Phytoplankton photoacclimation and photoadaptation in response to environmental gradients in a shelf sea. *Limnol. Oceanogr.* 51:936–49.

Mortain-Bertrand, A. 1989. Effects of light fluctuations on the growth and productivity of Antarctic diatoms in culture. *Polar Biol.* 9:245–52.

Pahl-Wostll, C. & Imboden, D. M. 1990. DYPHORA—a dynamic model for the rate of photosynthesis of algae. *J. Plankton Res.* 12:1207–21.

Palmisano, A. C., Soohoo, J. B., Soohoo, S. L., Kottimeier, S. T., Craft, L. L. & Sullivan, C. W. 1986. Photoadaptation of *Phaeosystis pouchetii* advected beneath annual sea ice in McMurdo Sound, Antarctica. *J. Plankton Res.* 8:891–906.

Price, N. M., Harrison, G. I., Hering, J. G., Hudson, R. J., Nirel, P. M. V., Palenik, B. & Morel, F. M. M. 1989. Preparation and chemistry of the artificial algal culture medium Aquil. *Biol. Oceanogr.* 6:443–61.

Riegger, L. & Robinson, D. 1997. Photoinduction of UV-absorbing compounds in Antarctic diatoms and *Phaeocystis antarctica. Mar. Ecol. Prog. Ser.* 160:13–25.

Robinson, D. H., Arrigo, K. R., DiTullio, G. R. & Lizotte, M. P. 2003. Evaluating photosynthetic carbon fixation during *Phaeocystis antarctica* blooms. *In* DiTullio, G. R. & Dunbar, R. B. [Eds.] *Biogeochemistry of the Ross Sea.* AGU Antarctic Research Series, Wahington, D.C., pp. 77–92.

Ross, O. N., Moore, C. M., Suggett, D. J., MacIntyre, H. L. & Geider, R. J. 2008. A model of photosynthesis and photo-protection based on reaction center damage and repair. *Limnol. Oceanogr.* 53:1835–52.

Roy, T., Rayner, P., Matear, R. & Francey, R. 2003. Southern Hemisphere ocean CO_2 uptake: reconciling atmospheric and oceanic estimates. *Tellus Ser. B Chem. Phys. Meteorol.* 55:701–10.

Saggiomo, V., Catalano, G., Mangoni, O., Budillon, G. & Carrada, G. C. 2002. Primary production processes in ice-free waters of the Ross Sea (Antarctica) during the austral summer 1996. *Deep-Sea Res. Part II Top. Stud. Oceanogr.* 49:1787–801.

Schloss, I. & Estrada, M. 1994. Phytoplankton composition in the Weddell-Scotia confluence area during austral spring in relation to hydrography. *Polar Biol.* 14:77–90.

Schoemann, V., Becquevort, S., Stefels, J., Rousseau, W. & Lancelot, C. 2005. *Phaeocystis* blooms in the global ocean and their controlling mechanisms: a review. *J. Sea Res.* 53:43–66.

Smith, W. O., Dennett, M. R., Mathot, S. & Caron, D. A. 2003. The temporal dynamics of the flagellated and colonial stages of *Phaeocystis antarctica* in the Ross Sea. *Deep-Sea Res. Part II Top. Stud. Oceanogr.* 50:605–17.

Tagliabue, A. & Arrigo, K. R. 2005. Iron in the Ross Sea: 1. Impact on CO2 fluxes via variation in phytoplankton functional group and non-Redfield stoichiometry. *J. Geophys. Res. Oceans* 110:C03009, doi:10.1029/2004JC002531.

Takahashi, T., Sutherland, S. C., Sweeney, C., Poisson, A., Metzl, N., Tilbrook, B., Bates, N., et al. 2002. Global sea-air CO_2 flux based on climatological surface ocean pCO(2), and seasonal biological and temperature effects. *Deep-Sea Res. Part II Top. Stud. Oceanogr.* 49:1601–22.

Vaillancourt, R. D., Marra, J., Barber, R. T. & Smith, W. O. 2003. Primary productivity and in situ quantum yields in the Ross Sea and Pacific Sector of the Antarctic Circumpolar Current. *Deep-Sea Res. Part II Top. Stud. Oceanogr.* 50:559–78.

Van de Poll, W. H., Van Leeuwe, M. A., Roggeveld, J. & Buma, A. G. J. 2006. Nutrient limitation and high irradiance acclimation reduce PAR and UV-induced viability loss in the Antarctic diatom *Chaetoceros brevis* (Bacillariophyceae). *J. Phycol.* 41: 840–50.

Van de Poll, W. H., Visser, R. J. W. & Buma, A. G. J. 2007. Acclimation to a dynamic irradiance regime changes excessive irradiance sensitivity of *Emiliania huxleyi* and *Thalassiosira weissflogii*. *Limnol. Oceanogr.* 54:1430–8.

Van Hilst, C. M. & Smith, W. O. 2002. Photo synthesis/irradiance relationships in the Ross Sea, Antarctica, and their control by phytoplankton assemblage composition and environmental factors. *Mar. Ecol. Prog. Ser.* 226:1–12.

Van Leeuwe, M. A. & Stefels, J. 2007. Photosynthetic responses in *Phaeocystis antarctica* towards varying light and iron conditions. *Biogeochemistry* 83:61–70.